

# Irreversible polymer adsorption from semidilute and moderately dense solutions

Richard Zajac and Amitabha Chakrabarti

*Department of Physics, Kansas State University, Manhattan, Kansas 66506*

(Received 21 February 1995)

We present results from a Monte Carlo study of polymer adsorption from solution at a solid-liquid interface, in the limit of infinitely large adsorption energy. We study the kinetics of adsorbed layer formation for both the cases of end-functionalized chains and homopolymers. In the former case, the adsorbed layer is found to be in the “brush” regime described by Milner, Witten, and Cates [Macromolecules **21**, 2610 (1988)], and its growth is consistent with the formation of an activation barrier, as predicted by Ligoure and Leibler [J. Phys. (Paris) **51**, 1313 (1990)]. In the latter case, the resulting “pancake” layer is analyzed in terms of loop, train, and tail distributions. The results are compared with recent scaling arguments proposed by Guiselin [Europhys. Lett. **17**, 225 (1992)].

PACS number(s): 61.25.Hq, 36.20.Ey, 68.45.Da, 82.70.-y

## I. INTRODUCTION

Systems of polymer chains at an interface have received considerable attention recently. Indeed, such polymer systems have proven useful in many applications, such as colloidal stabilization and lubrication [1]. The behavior of polymer chains in such systems strongly depends on their conformation at the surface. Computer simulation provides a powerful tool for studying these conformations and their dependence on physical conditions. Most of the previous simulation studies have considered either reversibly adsorbed layers [3–6] or grafted layers [2] with preassigned values of the surface coverage. Much less is known about *irreversible* adsorption of polymers onto a solid-liquid interface, although such systems have attracted recent attention from both theorists [7–9] and experimentalists [10–13].

For the case of end-functionalized chains grafted onto a flat surface, the self-consistent-field (SCF) theory of Milner, Witten, and Cates (MWC) predicts a parabolic form for this profile [14], unlike the step-function form assumed by Alexander [15] and de Gennes [16]. The assumption of a parabolic form for this profile has then served as the starting point for some analytical studies of the adsorption kinetics [17]. This assumption is appropriate to a regime where the chains are strongly stretched; however, it may not be applicable (or even attainable) for the growth of a layer where screening by the free chains is important [18]. Indeed, for reversible adsorption of end-functionalized chains, it has been shown that for moderate adsorbing strengths penetration of the free chains into the adsorbed phase can lead to a screening of the interaction between adsorbed chains, altering the form of the adsorption profile throughout the adsorption process [4]. It is therefore of interest to follow the growth of such a layer from solution for a very large adsorption energy where the screening effects of the free chains are expected to be small, and the end-functionalized chains could achieve the parabolic regime.

For the case of homopolymer adsorption, previous theoretical studies of irreversible adsorption have been per-

formed by Guiselin [7] and Aubouy and Raphaël [8]. In these studies, the time required to saturate the adsorbing surface is assumed to be very short, so that the adsorbed layer is formed instantaneously from a concentrated bulk solution or a melt. Only those chains which are touching the surface at that given instant are kept, and are taken to be irreversibly adsorbed. Recent experimental studies [12,13] have also been carried out to study irreversible adsorption of poly(dimethylsiloxane) (PDMS) on porous silica from a concentrated solution of dichloromethane or from melts. The results of these experiments seem to agree with theoretical arguments in the limit of very large solution concentrations or melts. However, all details of the adsorption process are neglected in these theoretical and experimental studies, and only the final conformation is studied.

In this paper, we study the growth of polymer layers from solution for the case where the chains become irreversibly adsorbed. We examine the cases of both homopolymer adsorption and end-functionalized polymer adsorption. The monomer concentrations considered in our studies range from semidilute to moderately dense. For these concentrations, the adsorbed layer does not form instantaneously and the theoretical arguments mentioned above are not directly applicable. In our simulations, we characterize both the kinetics of the layer formation and the conformation of the chains in the layer at various stages of the growth process. The results are then compared with applicable theoretical arguments.

The remainder of this paper is organized as follows. In Sec. II we describe our model and the method of simulation used in this study. In Sec. III we present results for the adsorption of end-functionalized chains. In Sec. IV we present results for the adsorption of homopolymers. The results of these studies are compared with previous studies wherever possible. In Sec. V we summarize our results and discuss them briefly.

## II. MODEL AND NUMERICAL METHODS

We model the polymer chains as mutually self-avoiding random walks of  $N - 1$  steps, on a three dimensional

$50 \times 50 \times 100$  cubic lattice. The self-avoidance criterion produces an excluded volume interaction between monomers, characteristic of a good solvent. We place a number of such chains in the system to make up the desired bulk concentration of monomers,  $\phi_0$ , taking care not to place a monomer at a lattice site which is already occupied. Lattice sites not occupied by monomers correspond to solvent molecules. We consider chain lengths of  $N = 50, 100,$  and  $200$  monomers (49, 99, and 199 steps, respectively), in solutions of monomer concentration of 5%, 10%, and 20%. The system boundaries are periodic in the  $x$  and  $y$  directions, while the  $z = 0$  and  $z = 99$  boundaries are taken to be impenetrable surfaces. The wall-to-wall distance in the  $z$  direction is much larger than the expected layer thickness for the chain lengths considered, so that the wall at  $z = 99$  should not affect a layer formed at the  $z = 0$  wall. Our results in Secs. III and IV confirm this. The system of chains is made to evolve by repeatedly choosing a monomer at random, and attempting a random move with that monomer. Possible moves include kink jumps, end wiggles, crank-shaft turns, and a slithering motion loosely called a "reptation" of the chain, weighted so that half of the attempted moves are reptations [19]. For initial equilibration of the system in an athermal solvent, the test move is accepted if it does not cause two monomers to overlap, or to cross an impenetrable surface. After this period of initial equilibration, an irreversible contact interaction is "turned on" at the  $z = 0$  surface. Thereafter, any test move which requires an adsorbing monomer to be detached from this surface is rejected. The adsorbing monomers may be the first monomers of the chains only (end-functionalized case), or all monomers (homopolymer adsorption). We measure time  $t$  in units of Monte Carlo steps per monomer (MCS/M), such that one MCS/M corresponds to as many move attempts as there are monomers. In this way, each monomer undergoes an average of one trial move during one MCS/M, although not every monomer will necessarily be chosen for an attempted move during one MCS/M. It should be noted that the irreversible interaction leads to a difference in the chain dynamics from previous studies with finite surface interactions. In the present case, sliding of an adsorbed monomer along the adsorbing surface is not allowed, since we are presumably modeling a chemical (fixed) bond [20]. Such chemical bonds have a strong directional preference and therefore resist lateral movement (sliding) of the bound monomers. In particular, an adsorbed chain is no longer free to reptate onto and along the surface. In the case of end-functionalized chains this may cause the absence of a mode of oscillation wherein an adsorbed chain is continually reeled in and out, perpendicularly to the surface. Its effect on the adsorption density profile will be addressed later.

The interaction with the adsorbing surface causes the gradual buildup of a layer at  $z = 0$ , similar to that depicted in Fig. 1 of Ref. 4. In order to maintain a constant monomer concentration in the bulk, every time a chain becomes adsorbed we attempt to place a new chain on the lattice at some random location. If the attempt fails,

we try again at a new randomly chosen location. In order to ensure that this placement of a new chain does not affect the growth kinetics, we place the new chain such that its center of mass lies in the half of the system furthest from the adsorbing surface. We have verified that the resulting density profiles are well behaved around  $z = 50$  (i.e., the midway point), to ensure that our method of placing chains does not cause any peculiarities in the chemical potential. In this way, we model a system which is in diffusive contact with a reservoir, which can supply chains without limit to maintain an approximately constant chain density far from the surface (provided that the volume of the bulk phase does not change appreciably). This mimics the effect of a fixed chemical potential far from the surface, in the bulk phase. The diffusive contact with the surface phase then causes equalization of the surface to the equivalent value of this fixed chemical potential. The total number of chains in the system is therefore not constant, but varies continually. This open-system approach is strictly more accurate than the closed-system approaches, which are more prone to finite-size effects. In particular, the behavior of the growth kinetics of these closed systems is quickly cut off as the finite bulk solution becomes depleted (see, for example, Ref. [5]). Despite these efforts, it will be seen that the bulk concentration does in fact increase slightly due to an exclusion of the free chains from an adsorption region near the surface.

The system thus evolves toward a final "quasiequilibrium" configuration while physical quantities of interest are measured. This process is then repeated several times with different random initial conditions, and the results of the measurements are averaged over all the "runs" (typically, we average over ten runs for each system configuration). By this averaging we obtain quite accurate results for the kinetics of layer growth.

### III. ADSORPTION OF END-FUNCTIONALIZED CHAINS

#### A. Growth kinetics

Presently, we consider the case of polymer chains of which only the first monomer adsorbs irreversibly to the  $z = 0$  surface, i.e., molecules with a functionalized "sticker" head. In Figs. 1 we plot the surface density of adsorbing heads  $\sigma$  as a function of time for a typical system configuration. At early times,  $\sigma$  can be seen to grow according to a power law, consistent with Brownian diffusion of the chains toward the surface [Fig. 1(a)]. The exponent, however, is not 0.5, as expected, but around 0.3 (although the first few data points would tend to yield a larger exponent). The slowing down of this power-law growth is attributed to screening by the chains already present at the surface [17], which begin to form a layer before even the first measurement is made. Even in the cases of a 5% solution, we note that there are already over 1000 monomers in the adsorbed phase at the time of our

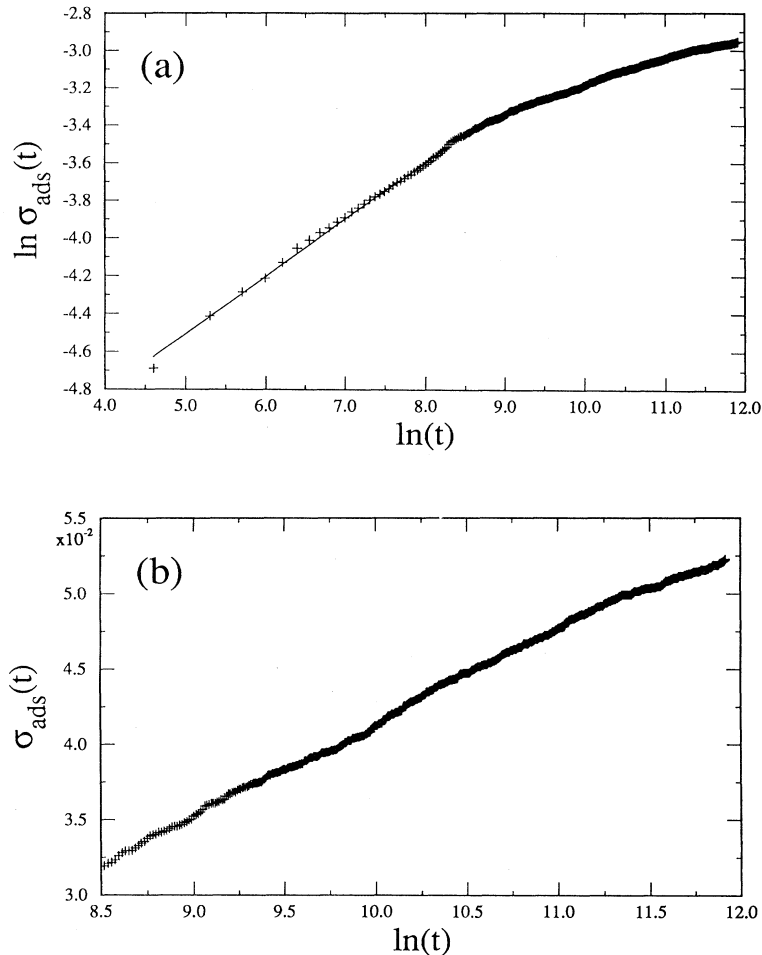


FIG. 1. Growth of the surface density of adsorbing monomers,  $\sigma$ , with time  $t$  for the case of end-functionalized chains,  $N = 100$ ,  $\phi_0 = 10\%$ . (a)  $\ln(\sigma)$  vs  $\ln(t)$ : note the power-law growth at early times. (b)  $\sigma$  vs  $\ln(t)$ : note the logarithmic behavior at late times.

first measurement ( $t = 100$  MCS/M). From Fig. 1(a), a crossover is evident at intermediate times, at which point the power-law behavior gives way to a slower growth. At late times [Fig. 1(b)], the growth of  $\sigma$  is seen to be essentially logarithmic in  $t$ . This logarithmic growth is characteristic of the second phase of growth; it arises with the formation of a strongly stretched brush layer. Because of this layer, an adsorbing chain must give up some of its free energy in straightening itself out to penetrate the brush layer. In this way, adsorption of further chains is impeded by the formation of an activation barrier, as described by Ligoure and Leibler. We can quantify this logarithmic growth in terms of a characteristic grafting density  $\sigma^*$  such that  $\sigma(t) \sim \sigma^* \ln(t)$ . In Table I, we list the values of  $\sigma^*$  obtained from least-squares fits of  $\sigma(t)$ , for the system configurations considered. We note that  $\sigma^*$  decreases with increasing chain length, scaling roughly as  $\sigma^* \sim 1/N$ . We have verified that the form of Ligoure and Leibler for this growth shows a similar behavior. The activation barrier is thus more effective at impeding the progress of longer chains through the brush. It does not, however, appear to change with changing solution concentrations, remaining practically constant for

all concentrations considered.

We have not pursued the study of the growth kinetics past the point where the onset of this second phase of growth has been clearly established. Indeed, achieving a final steady state is not practical for such a system. Since the chain exchange can only be one sided, there can be no equilibrium governed by a detailed balancing of chains.

TABLE I. Characteristics of a growing brush layer of end-functionalized chains. Values correspond to an instantaneous, averaged “quasiequilibrium” state (see text).

$N$	$\phi_0^{\text{actual}}$	$\sigma^*$	$\sigma_{\text{quasiequil}}$	$\phi_{\text{max}}$	$\langle z \rangle_{\text{ads}}$	$\frac{\langle z \rangle_{\text{ads}}}{\sigma^{1/3} N}$
50	0.062	0.0132	0.075	0.305	6.43	0.305
50	0.122	0.0128	0.093	0.354	6.75	0.298
50	0.242	0.0188	0.122	0.439	7.09	0.286
100	0.063	0.00545	0.039	0.191	10.25	0.301
100	0.132	0.00579	0.052	0.264	10.58	0.283
100	0.264	0.00781	0.078	0.370	10.87	0.254
200	0.0823	0.00284	0.022	0.155	16.15	0.286
200	0.1539	0.00352	0.032	0.219	15.89	0.249

### B. Layer structure

As explained above, the growth of the adsorbed layer was terminated after the onset of the logarithmic phase was evident. The system configurations thus achieved therefore only correspond to a “quasiequilibrium” situation. While we would expect the further growth of the layer to proceed indefinitely (barring effects due to a finite-sized system), we do not expect the chain conformations to change appreciably. We therefore average our system conformations over late times (logarithmic phase)—typically over a time  $t = 10\,000$  MCS/M—in order to describe the structure of the layer in this phase of growth. The density profiles of a typical system averaged in this way are plotted in Fig. 2. The density profile of adsorbed chains resembles a parabola [14], motivating a least-squares fit to the functional form  $\phi_{ads}(z) = A - Bz^2$  which is also shown in Fig. 2. We also calculate  $\langle z \rangle$ , the first moment of the brush layer. From this, we find that  $\langle z \rangle / \sigma^{1/3} \sim N$ , as evidenced in Table I where we see that the ratio  $\langle z \rangle / \sigma^{1/3} N$  is approximately constant. This scaling result is characteristic of a strongly stretched brush [14–16]. We note a tendency for this ratio to decrease slightly as the bulk concentration increases. The stronger osmotic pressure of a more dense solution compresses the layer and reduces  $\langle z \rangle$ . As well, a MWC parabola obeys the relation [14,21]

$$\frac{4A^3}{9BN^2\sigma^2} = 1, \quad (1)$$

which we find to be in good agreement with the results of our parabolic fits. From these results, we can also deduce the value of the excluded volume parameter  $\omega$  according to the relations

$$\omega = \frac{9\pi^2\sigma^2}{32A^3} \quad \text{or} \quad \omega = \frac{\pi^2}{8N^2B}. \quad (2)$$

From these two relations we obtain  $\omega \approx 0.5$ , particularly for the low concentration cases, where the parabolic fit is especially good. This value of  $\omega$  is in agreement with previous studies of end-grafted lattice polymers in the absence of any free chains [21]. This result indicates that

the screening effect of the free chains (which would result in a smaller value for the effective excluded volume parameter) is small in the present simulations.

The above conclusion is supported by noting that the free chain density quickly vanishes within the layer. The free chains are almost totally expelled from the adsorbed phase, in contrast to our previous study of finite adsorption energies which showed significant penetration by the free chains down to the adsorbing surface [4]. Because of this expulsion of the free chains from the adsorbed phase, the actual monomer concentration in the bulk solution,  $\phi_0^{actual}$ , is slightly larger than our initial concentration  $\phi_0$ . By our adding new chains to the system to prevent depletion of the solution, we are maintaining the number of free chains in the whole system; but the volume this number is restricted to becomes smaller as the adsorbed phase grows, so  $\phi_0^{actual}$  is slightly greater than  $\phi_0$ . Of course, this effect will be weak when the volume of the system is much larger than the volume of the final layer. In this way, the increase in bulk concentration is an artifact of our finite-sized model. The measured values of  $\phi_0^{actual}$  are also presented in Table I, where we can see that the increase in concentration from the intended values (see Sec. II) is small, but non-negligible.

In Fig. 3(a) we plot the density of monomers in the adsorbed phase scaled by its maximum value,  $\phi_{ads}(z)/\phi_{max}$ , as a function of the reduced distance,  $z/\langle z \rangle$ , for the various cases considered. We also plot the reduced density profile of free monomers,  $\phi_{free}(z)/\phi_0^{actual}$ . The resulting density profiles are seen to coincide, leading us to infer the scaling relations

$$\phi_{ads}(z) = \phi_{max} g\left(\frac{z}{\langle z \rangle_{ads}}\right), \quad (3)$$

$$\phi_{free}(z) = \phi_0 f\left(\frac{z}{\langle z \rangle_{ads}}\right), \quad (4)$$

where we might expect that

$$g(z) + h(z) \approx 1. \quad (5)$$

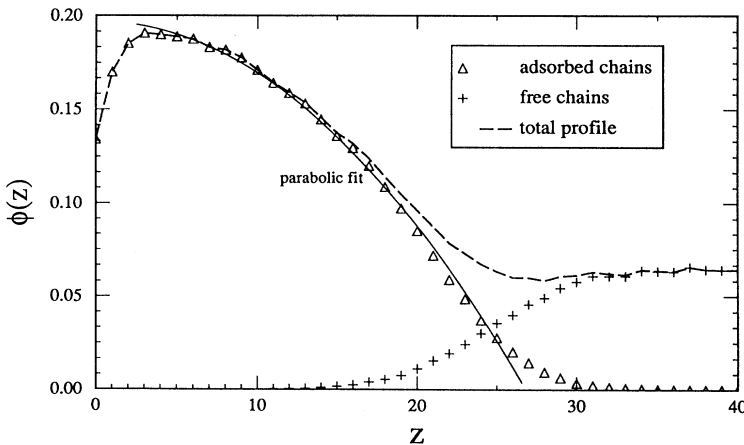


FIG. 2. Density profile of monomers near the surface for the case of end-functionalized chains,  $N = 100$ ,  $\phi_0 = 5\%$ . The solid line is a least-squares fit to the functional form  $\phi = A - Bz^2$ . Note the almost complete expulsion of the free chains from the brush region.

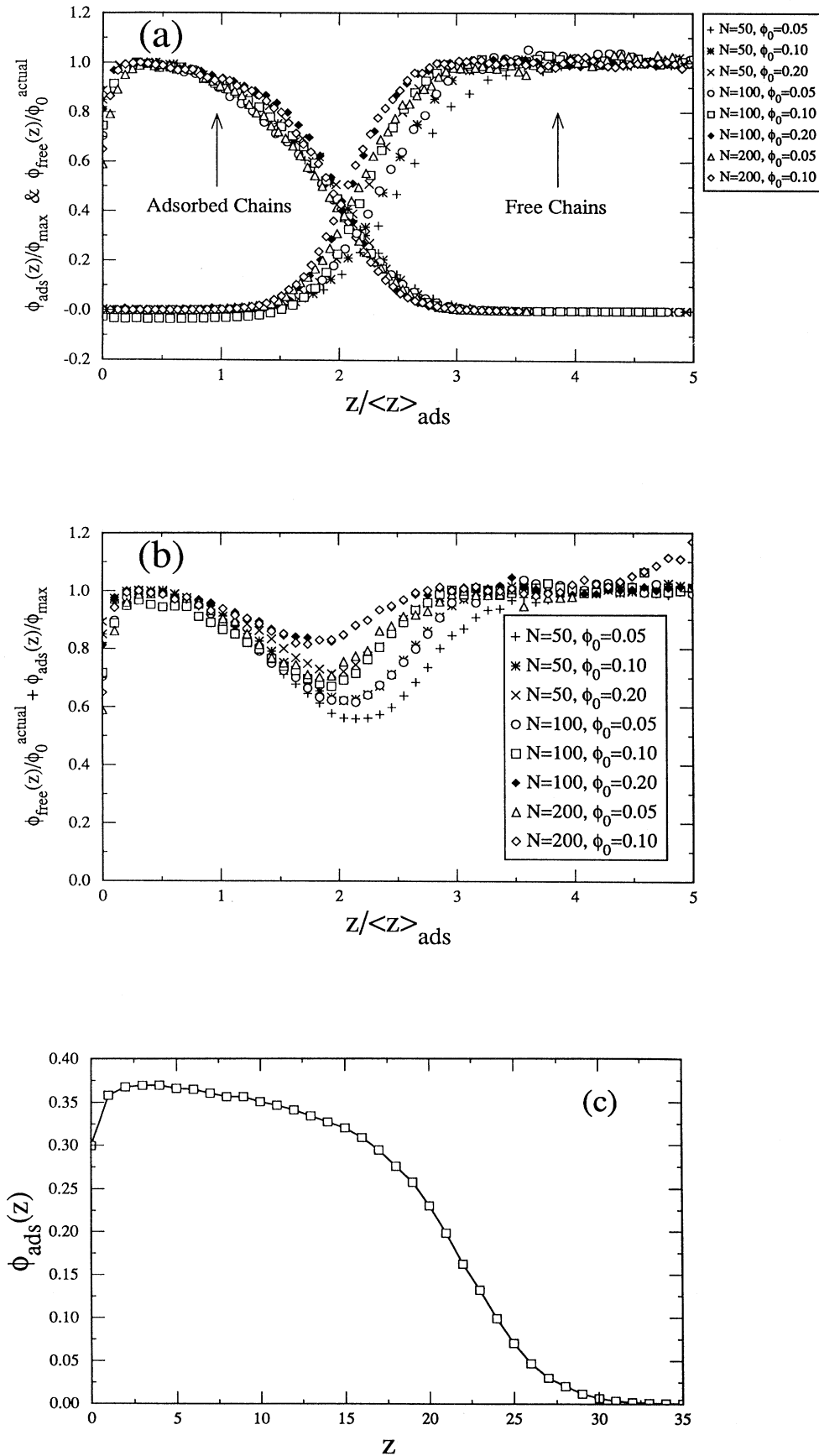


FIG. 3. Scaling plot of the density profile for the case of end-functionalized chains. (a) Adsorbed chain profile scaled by  $\phi_{ads}^{max}$ ; free chain profile scaled by  $\phi_0^{actual}$ . All  $z$  distances are scaled by  $\langle z \rangle_{ads}$ . (b) Sum of the scaled profiles:  $\phi_{ads}(z)/\phi_{ads}^{max} + \phi_{free}(z)/\phi_0^{actual}$ . All  $z$  distances are scaled by  $\langle z \rangle_{ads}$ . (c) Density profile of adsorbed chains for  $N = 100, \phi_0 = 0.2$ . Note the flattening out of the parabola at higher densities.

The latter relation can be understood as expressing the constancy of the chemical potential  $\mu(z)$  at quasiequilibrium, assuming that  $\mu$  is proportional to both  $\phi_{ads}$  and  $\phi_{free}$ , i.e.,  $\mu(z) = A_0\phi_{ads}(z) + B_0\phi_{free}(z)$ . Far from the surface,  $\phi_{free} = \phi_0$  and  $\phi_{ads} = 0$ , while right by the surface,  $\phi_{free} = 0$  and  $\phi_{ads} = \phi_{max}$ . We plot  $g + f$  in Fig. 3(b) and note that there is in fact a significant dip in the region where the bulk and adsorbed phases interact, presumably due to screening of their self-interactions. We also note a trend for the dip to be more pronounced for shorter chain lengths. Shorter chains have a higher concentration of chain ends and are thus more interpenetrating. This in turn leads to stronger screening of their excluded volume interactions and a larger deviation of  $g + f$  from unity. This deviation may therefore be seen as an effect of finite chain lengths. On the other hand, we must also bear in mind that our system is not at equilibrium; the constancy of  $\mu$ , however, is only strictly true for an equilibrium situation. It is therefore possible that the system's evolution is not quasistatic, causing the dip in  $\mu$ . Finally,  $\mu$  may not be simply a linear function of  $\phi$ ; it may be that this moderately dense system requires a more complex equation of state.

Although the scaled parabolas seem to coincide reasonably well [Fig. 3(a)], there is a visible tendency for the profiles from higher concentrations to flatten out

more at larger  $z/\langle z \rangle$ . In particular, for the case of  $N = 100$ ,  $\phi_0 = 20\%$  [Fig. 3(c)], a small plateau region becomes visible in the "parabola," as the higher osmotic pressure of the bulk causes the chain distribution to become slightly more compact and to deviate from the parabolic form. This flattening out of the parabola at higher concentrations has been predicted by Shim and Cates [22], who have generalized the MWC self-consistent-field approach to the case of dense systems of grafted chains. They applied a Flory-Huggins type equation of state, which allows for saturation effects at high densities, and considered an extra non-Gaussian term for the chain elasticity, in order to prevent unphysical extension of the chains at these higher densities. At low densities they recovered the MWC parabolic profile, but the profile was seen to flatten out as the grafting density was increased to moderate values. If the equation of state does in fact cross over to a nonquadratic form, i.e., where the free energy is not proportional to  $\phi^2$ , then we cannot expect  $\mu$  to be linear in  $\phi(z)$ , and Eq. (5) no longer holds.

We now compare the density profile of an irreversible adsorption case in quasiequilibrium to that of a  $\Delta = 6kT$  case in true equilibrium [Fig. 4(a)], both with roughly the same adsorbance (i.e., the same total number of monomers in the adsorbed phase) and bulk concentra-

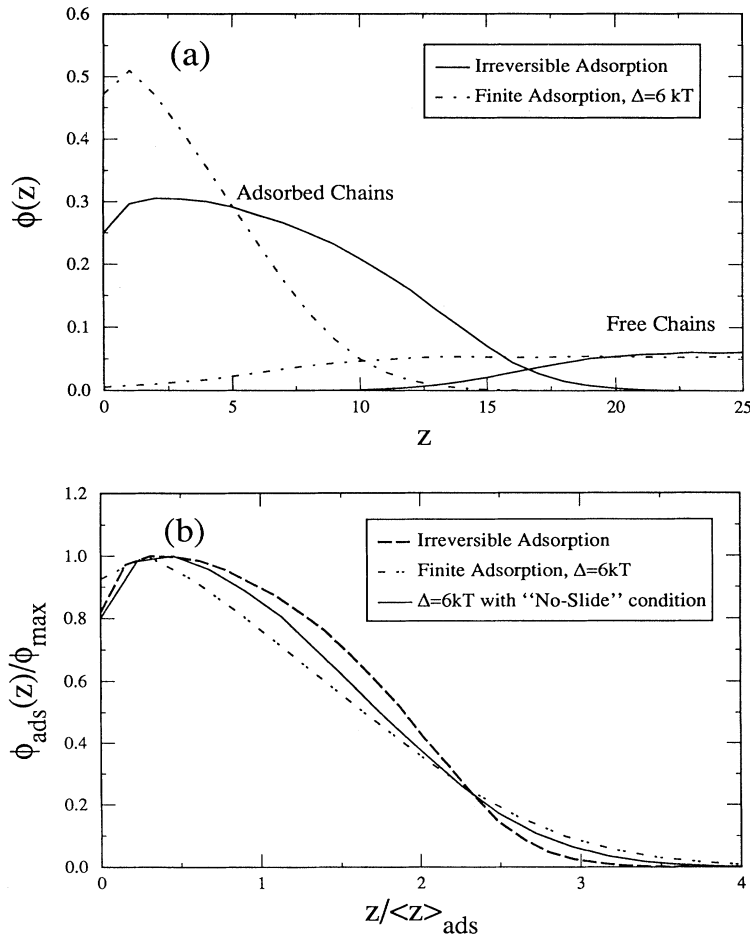


FIG. 4. Comparison of density profiles of irreversible ( $\Delta = \infty$ ) and reversible ( $\Delta = 6kT$ ) end adsorption. (a) Equilibrium profiles of cases with similar bulk concentrations  $\phi_0 \approx 0.05$  and similar adsorbances  $\Gamma$ . (b) Comparison of scaling functions for irreversible ( $\Delta = \infty$ ) and reversible ( $\Delta = 6kT$ ) end adsorption. The results for  $\Delta = 6kT$  are taken from Ref. [4]. The solid line represents a reversible adsorption ( $\Delta = 6kT$ ) case where adsorbed monomers are not allowed to slide along the surface.

tion. We find that the value of  $\phi_{ads}(z=0)$  is much larger for the latter case; the adsorbed chains are more stretched in the case of irreversible adsorption. While both cases have about the same number of adsorbed chains, a greater portion of the chains is pressed against the surface in the case of finite adsorption strength. In the limit of irreversibly strong adsorption, the functional tips are apparently very successful at driving the non-adsorbing monomers off the surface. Now in our previous study [4], we found that the density profiles of various systems with  $\Delta = 6kT$  and  $\Delta = 9kT$  obeyed a scaling relation similar to Eq. (3). When rescaled as above, these profiles were found to coincide with a common scaling function. One might therefore question whether Eq. (3) is valid for all values of  $\Delta$ , from low values up to and including the present case of  $\Delta = \infty$ . It turns out, however, that the scaling functions  $g(z)$  and  $f(z)$  are not the same as those in our previous study; these two studies take place in different regimes, so the scaling functions are naturally different. This is demonstrated in Fig. 4(b) where we compare  $g(z)$  with the scaling function derived in Ref. [4]. We see that there is a small but definite difference in the scaling functions. Furthermore, we compare these two functions with a third, derived from a model similar to that of Ref. [4], i.e., with a finite adsorption energy ( $\Delta = 6kT$ ), for  $N = 50$ ,  $\phi_0 = 0.05$ , but with the artificially imposed condition that there be no “sliding” of adsorbing monomers at the surface. This mimics the chain dynamics of the present irreversible study to some extent. The resulting scaling function can be seen to lie between the two other functions, without coinciding with either one. It is interesting to note that this “hybrid” function can also be fitted to a parabolic form whereas the original, “with-sliding” function has a Gaussian shape. The fit, however, is much worse in the tail region of the profile than it is for the irreversibly adsorbed chains, since the change in dynamics mostly affects the proximal region of the density profile. Presumably, a strong lateral anchoring of the grafting monomers helps the chains to stretch out, resulting in a more parabolic profile. Interestingly, most of the

previous studies which consider only end-grafted chains without chain exchange and which yield parabolic profiles consider the head group to be immovable. In this way, they too provide this strong anchoring against lateral motion. It should be noted that Lai and Binder [23] did not find any such difference between their so-called “quenched” and “annealed” states, although they only looked at grafted chains with an infinite  $\Delta$  in the absence of any free chains. In our case, artificially imposing this “no-slide” condition provides a strong lateral anchoring, but it does not produce the expulsion of free chains, and thus cannot exactly match the scaling functions obtained in the irreversible case. In fact, the imposition of this condition does not seem to affect the free chain density profile at all. The imposition of the “no-slide” condition on the case of finite  $\Delta$  reduces the equilibrium value of  $\phi_{ads}(z=0)$ , but it also drastically reduces the total adsorbance. It is easier to pack more chains into the adsorbed phase when they can easily redistribute themselves along the surface. We conclude that it is only in the case of a finite adsorption energy that the entropy difference caused by this lateral freedom significantly affects the form of the density profile. For irreversible cases, the change in dynamics only perturbs the parabolic fit slightly, although the kinetics will no doubt be speeded up if the chains can diffuse along the surface.

We present a similar scaling study in Fig. 5, where the reduced density profiles are plotted for different times within a given system configuration. We see that the scaling relations given by Eqs. (3) and (4) are obeyed dynamically as well. We conclude that  $\langle z \rangle$  can be considered the dominant length scale in the profile, throughout the growth of the layer.

## IV. ADSORPTION OF HOMOPOLYMER CHAINS

### A. Growth kinetics

We now investigate the formation of a polymer layer in the case where all monomers can interact irreversibly

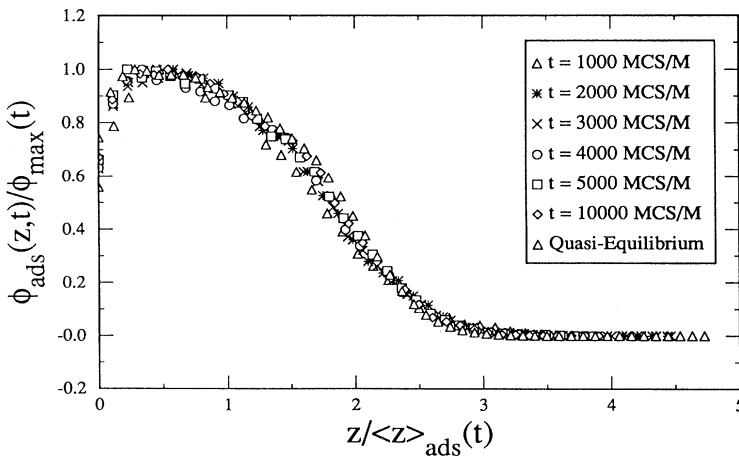


FIG. 5. Dynamic scaling plot of scaled  $\phi_{ads}(z)$  for the case of end-functionalized chains,  $N = 100$ ,  $\phi_0 = 10\%$ . The adsorbed chain profile is shown instantaneously scaled by  $\phi_{ads}^{\text{max}}$  at various times  $t$  (measured in units of Monte Carlo steps per monomer, as defined in the text). The distances are similarly instantaneously scaled by  $\langle z \rangle_{ads}$ .

with the adsorbing surface. We define a quantity  $[1 - \theta(t)]$ , describing the surface density of free sites (here,  $\theta$  is the surface coverage of monomers). Initially, this quantity can be seen to decay exponentially with time, as shown in Fig. 6 where we plot its natural logarithm as a function of  $t$ . The decay constant  $\alpha$ , where  $(1 - \theta) \sim e^{-\alpha t}$ , is tabulated in Table II, for the various system configurations. From these values of  $\alpha$ , we note that  $\alpha \sim \phi_0/N^\nu$ , with  $\nu \approx 0.6$  ( $0.55 \pm 0.15$ , from a least-squares fit to our data). This exponential decay follows from considering the vacant sites as particles detaching from a surface. The probability  $\alpha$  of such a particle becoming detached is directly proportional to the number of monomers adjacent to the surface, into which the particle can “jump.” Now, if the polymer chains are initially viewed as spherical coils, then each coil will have a fraction  $f \sim aR^2/R^3 \sim a/R$  of its  $N$  monomers near the surface of the sphere. (Here,  $R$  is the radius of a spherical coil,  $a$  is the lattice constant, and  $A$  is the surface’s total area.) The number of such spheres centered between  $z = R/2$  and  $z = R/2 + a$  (and thus touching the surface) at  $t = 0$  is simply  $\phi_0 Aa/N$ , whence

$$\alpha \sim fN\phi_0 Aa/N \sim \phi_0 Aa/R \sim \phi_0 Aa/N^\nu, \quad (6)$$

which is the above result. Note that we use  $\phi_0$  rather than  $\phi_0^{actual}$  in this argument, since at early times the concentration of free chains has not increased significantly from its initial value  $\phi_0$ . This result suggests that the first phase of the growth of the polymer layer involves the gradual collapse of only those coils which are initially touching the surface. These are the same chains that are kept in Guiselin’s study [7]. The adsorption of further chains proceeds more slowly, requiring chain diffusion through the layer.

We consider the further growth of the whole layer by measuring  $\Gamma$ , the total amount of polymer in the adsorbed phase, in units of equivalent monolayers. In Fig. 7(a) we plot  $\ln(\Gamma)$  as a function of  $\ln(t)$  for a particularly illustrative system configuration. From it, we can see that the growth of the adsorbed phase follows a power law at early times. Again, this power is less than

TABLE II. Characteristics of a growing layer of homopolymer chains. Values correspond to an instantaneous, averaged “quasiequilibrium” state (see text).

$N$	$\phi_0$	$\alpha$	$z_{shift}$	$\Gamma_{tails}^{eff}$	$\frac{\alpha}{\phi_0 N^\nu}$
50	0.05	0.000437	3.70	4.54	0.0752
50	0.10	0.000881	3.92	6.31	0.0757
50	0.20	0.00139	4.92	3.62	0.0597
100	0.05	0.000305	6.09	7.98	0.0767
100	0.10	0.000501	6.56	8.49	0.0631
100	0.20	0.000893	5.48	10.33	0.0562
200	0.05	0.000219	9.34	14.96	0.0807
200	0.10	0.000401	11.73	10.81	0.0738

0.5, due to screening by the layer which is already significant by the time of the first measurement. We also plot  $\Gamma$  as a function of  $\ln(t)$  in Fig. 7(b), and see that at late times the growth of the adsorbed phase proceeds logarithmically, just as in the case of end-functionalized chains. As we shall see in the next section, the adsorbed layer has a stretched region similar to that of an end-adsorbed brush, which the incoming chains again can only penetrate by expending free energy to straighten out. Consequently, the same growth mechanism as described for end-adsorbing chains also applies here. During this logarithmic growth, the quantity  $(1 - \theta)$  defined above decays according to a power law (Fig. 8),  $(1 - \theta) \sim t^{-x}$ , where  $x$  depends on the chain length. For the shortest chains considered ( $N = 50$ ),  $x \approx 1$ , while for  $N = 100$  and  $200$   $x$  is much smaller (around 0.6). This linear behavior would seem to be due to a progressive adsorption of successive monomers along a chain, as each adsorbed chain is “reeled in.” This can only work with very short chains; longer chains form large loops which get entangled in the layer and slow down this “reeled in” process, as evidenced by decreasing values of  $x$  for longer chains. While this mechanism of adsorption is no doubt present at early times as well, it is only at late times that it becomes evident. This is because at these late times very few new chains are being added to the layer. While at early times the addition of new chains overwhelms the other con-

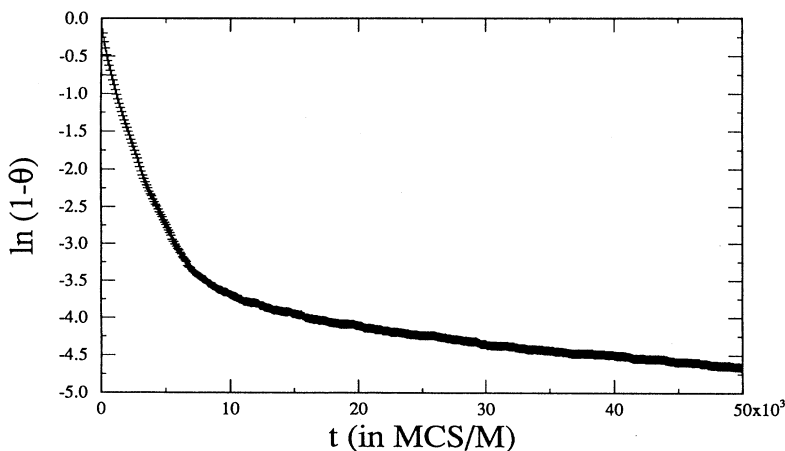


FIG. 6. Decay of the surface density of free sites with time for the case of homopolymer chains,  $N = 100$ ,  $\phi_0 = 10\%$ . Note that the initial decay of  $(1 - \theta)$  is exponential with time  $t$ .



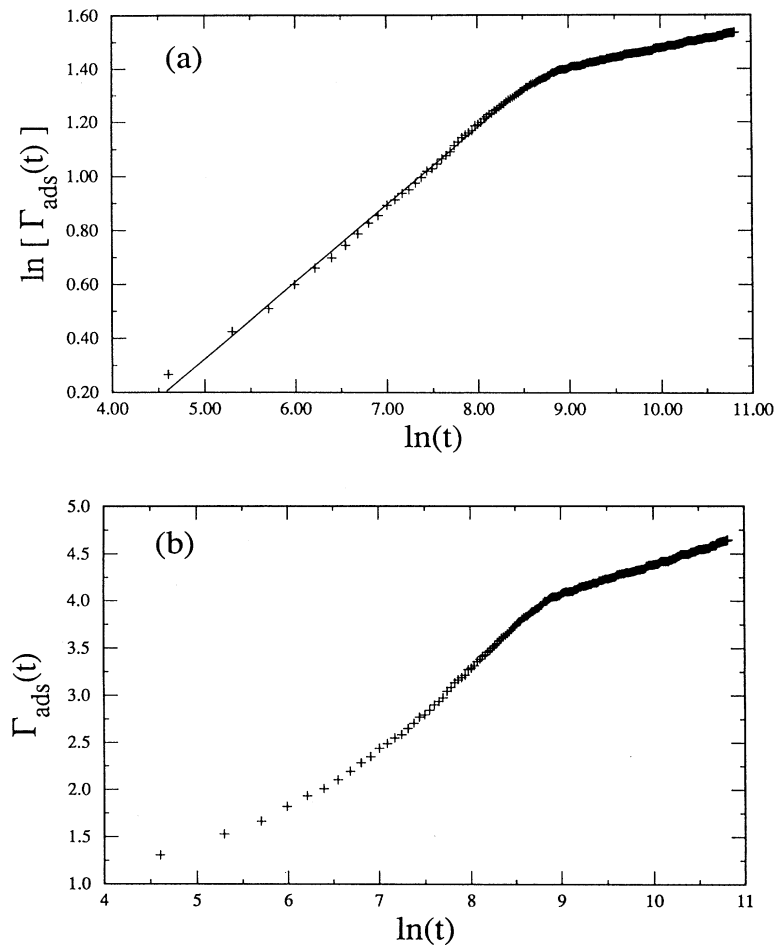


FIG. 7. Growth of the adsorbance  $\Gamma$  with time for the case of homopolymer chains,  $N = 100$ ,  $\phi_0 = 10\%$ . (a)  $\ln(\Gamma)$  vs  $\ln(t)$ : the initial growth proceeds according to a power law, slightly smaller than 0.5. (b)  $\Gamma$  vs  $\ln(t)$ : the growth at late times is essentially logarithmic.

tributions to the adsorption process, at late times the dominant mechanism is one involving a rearranging of the chains already in the adsorbed phase. Thus, this “reeling in” of the chains becomes visible at these late times.

### B. Layer structure

In Fig. 9, we plot the monomer density profiles near the surface, averaged over late times as in the case of end-functionalized chains. The surface is very nearly

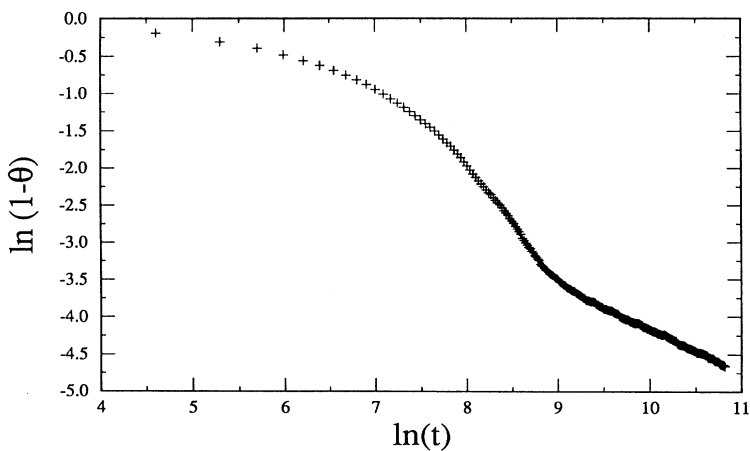


FIG. 8. Decay of the surface density of free sites with time for the case of homopolymer chains,  $N = 100$ ,  $\phi_0 = 10\%$ . Note how the decay obeys a power law at late times.

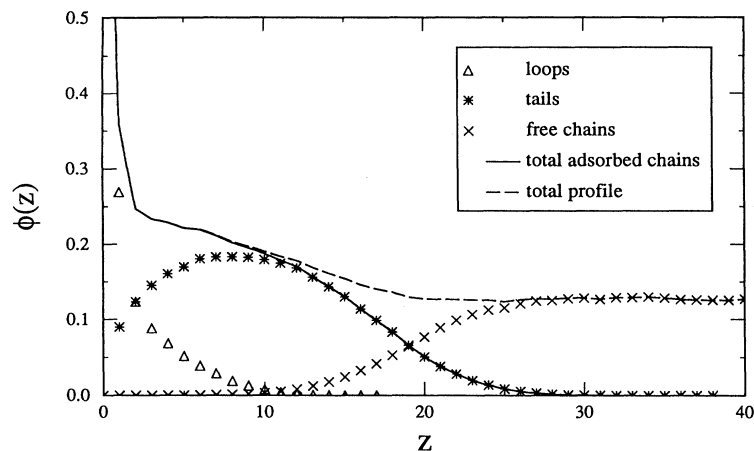


FIG. 9. Density profile of monomers near the surface for the case of homopolymer adsorption,  $N = 100$ ,  $\phi_0 = 10\%$ . The profile due to tails resembles a parabola, pushed outward by the dense layer of loops.

completely saturated, as witnessed by the sharp peak around  $z = 0$ . In the figure, we distinguish the profiles due to chain loops and tails. (The contribution from trains is trivial, residing purely at  $z = 0$ .) We note the rapid decay of the loop profile as we move away from the surface; beyond a few lattice spacings from the surface, only the tails are appreciably present. We therefore expect the interaction between adsorbed and bulk phases to occur primarily with the chain tails. The tail profile appears to be parabolic, as in the case of end adsorbed chains. Now, we might expect that the adsorbed chains be touching the surface at arbitrary points along the chain. The tails would then be of arbitrary lengths, making the tail brush polydisperse. But the density profile of a polydisperse brush is in general not parabolic [24]; the parabolic appearance therefore suggests that the

tail profile must be very nearly monodisperse. We verify this by plotting the distribution of tail lengths for a typical system in Fig. 10(a). From it, we can clearly see a sharp peak near  $N$ . The greatest contribution to the tail profile comes from chains with only a few monomers at one tip adsorbed. This is attributed to a dense protective layer at the surface which strongly favors penetration by one chain end, leading to only end adsorption of the chains. We have verified that this profile appears, albeit slightly distorted, as early as  $t = 1000$  MCS/M [see Fig. 10(b)], by which time over 60% of the surface sites are already occupied. Its form then quickly becomes more parabolic over a few thousand MCS/M, as the surface coverage increases, and the peak in the distribution becomes sharper. At this initial time,  $t = 1000$  MCS/M, the peak is broader and centered at smaller tail lengths,

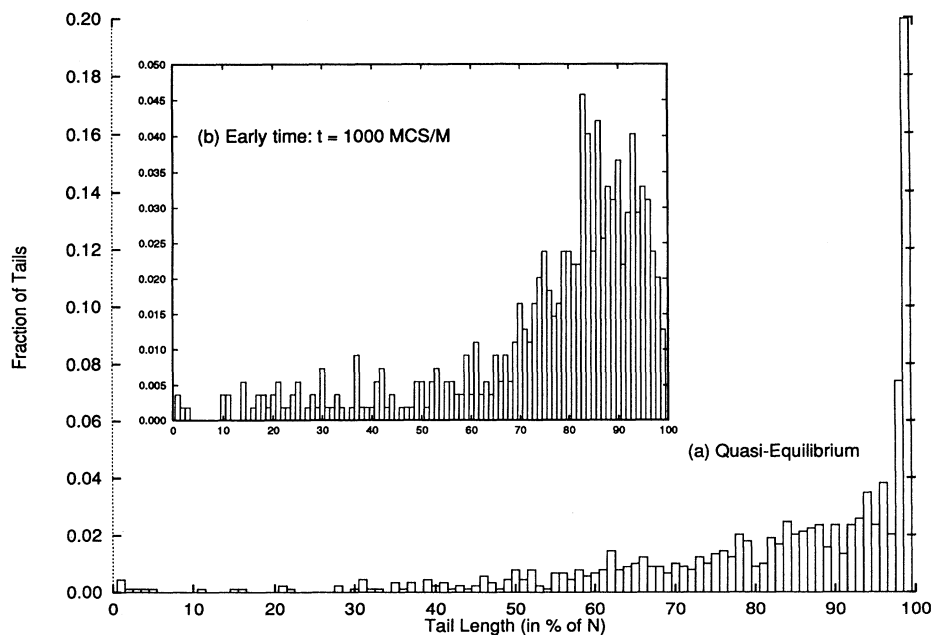


FIG. 10. Normalized distribution of tail lengths for the case of a homopolymer layer with  $N = 100$ ,  $\phi_0 = 10\%$ . (a) At quasiequilibrium: the strong peak near  $100\%N$  implies that the tails form a nearly monodisperse brush. Here, 892 tails were sampled. (b) The peak is present at early times, and is broader. Here, 546 tails were sampled.

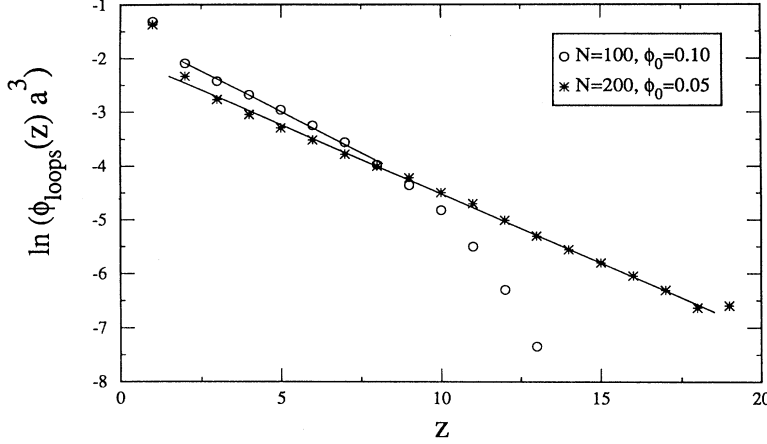


FIG. 11. Semilogarithmic plot of the density profile due to adsorbed loops, for the case of homopolymer adsorption. The profile decays exponentially with distance  $z$  in some region.

approximately  $0.85N$ . This is because the greater number of free surface sites allows for a larger portion of the chains' tips to adsorb, much like a diblock copolymer. We also note that, while the profile due to chains appears to be parabolic, the parabola can no longer be considered to be centered at the surface, as it was in the case of end-functionalized chains. Its center is displaced by the collapsed loops, a distance of several lattice spacings. This displacement,  $z_{shift}$ , is tabulated in Table II for the various system configurations, along with other profile parameters. By assuming that this is in fact a shifted MWC parabola, we can use Eq. (1) to infer an effective coverage  $\Gamma_{tails}^{eff}$  for the tails outside the loop region, which we include in Table II.

In Fig. 11 we plot the natural logarithm of  $\phi_{loops}$  as a function of  $z$ . From the figure, it can be seen that the profile due to loops decays exponentially in this limiting regime, apart from saturation effects near the surface and finite-chain-size effects at larger distances. We extract a characteristic decay length  $\lambda$ , such that  $\phi_{loops} \sim e^{-z/\lambda}$ , and find that in general  $\lambda/z_{shift} \approx 0.5$ . This supports the conclusion that the distribution of tails is "pushed" outward by the loops, as the peak of the tail parabola is shifted proportionately to  $\lambda$ .

For all the cases considered, we calculate and tabulate various quantities of interest in Table III. These include the average height of the layer  $\langle z \rangle$  and adsorbances contributed by the tails, loops, and tails of the layer. As

shown in this table, we can fit our results to the scaling form  $\langle z \rangle \sim \phi_0^b N^c$ . Guiselin [7] has proposed an elegant scaling argument to determine these exponents by analogy with the irreversibly adsorbed layer with a polydisperse brush formed from a melt, which we now summarize.

For a grafted polymer brush, we have from Alexander [15] that

$$\xi \sim \sigma^{-1/2}, \quad g \sim (a^2 \sigma)^{-5/6}, \quad (7)$$

where  $\xi$  is the blob size and  $g$  is the number of monomers per blob. For a polydisperse brush, let  $\mathcal{D}(n)$  be the number of pseudotails of length greater than  $n$ . (A long loop is considered to be two pseudotails.) Let us also assume that all pseudotails are stretched the same way, so that  $z = z(n)$ . Then, at a distance  $z$ , the layer can be seen as a brush of pseudotails with local grafting density  $\sigma(z) = \mathcal{D}(n(z))$ . Using this in Eq. (7), we find

$$\frac{dz}{dn} \sim \frac{\xi}{g} \sim a[a^2 \mathcal{D}(n)]^{1/3},$$

$$dz \sim a[a^2 \mathcal{D}(n)]^{1/3},$$

$$h \sim \int_0^N a[a^2 \mathcal{D}(n)]^{1/3}. \quad (8)$$

TABLE III. Characteristics of a growing layer of homopolymer chains. Values correspond to an instantaneous, averaged "quasiequilibrium" state (see text).

$N$	$\phi_0^{actual}$	$\langle z \rangle_{ads}$	$\frac{\langle z \rangle_{ads}}{(\phi_0^{actual})^{0.2} N^{0.81}}$	$\Gamma_{total}$	$\Gamma_{tails}$	$\Gamma_{loops}$	$\Gamma_{trains}$
50	0.059	3.39	0.251	2.954	1.327	0.632	0.995
50	0.116	3.93	0.254	3.543	1.909	0.637	0.997
50	0.230	4.55	0.257	4.566	2.953	0.615	0.999
100	0.064	5.86	0.244	3.572	1.918	0.666	0.988
100	0.127	6.86	0.249	4.605	2.900	0.714	0.990
100	0.228	7.48	0.241	5.986	4.169	0.823	0.994
200	0.077	10.85	0.248	4.667	3.054	0.633	0.981
200	0.146	11.93	0.240	6.373	4.642	0.748	0.982

Now let  $f(n)$  be the number of pseudetails of length  $n$  in a typical chain. For a melt, there will be  $\sim R\phi_0 \sim N^{1/2}$  monomers in the adsorbed phase per unit area, assuming that only the coils initially touching the surface are kept. This leads to the conditions

$$\int_1^N f(n)dn = N^{1/2},$$

$$\int_1^N nf(n)dn = N,$$

where the latter relation ensures that the typical chain has  $N$  monomers. Assuming that  $f(n)$  has the form of a power law, we find from these that  $f(n) \sim N^{1/2}n^{-3/2}$ . Using the fact that  $\mathcal{D}(n) = \int_n^\infty f(n) \sim n^{-1/2}$  in Eq. (8) yields

$$h \sim \int_0^N n^{-1/6} \sim N^{5/6} \quad (9)$$

for a layer formed in a melt. We can imagine our semidilute solution as a melt of blobs by making the substitutions  $N \rightarrow N/g_{sol}$  and  $a \rightarrow \xi_{sol}$ . As well, for a semidilute solution we have [25]  $\xi_{sol} \sim \phi_0^{-3/4}$  and  $g_{sol} \sim \phi_0^{-5/4}$ . Using this in Eq. (9) yields Guiselin's result, namely,

$$h \sim \phi_0^{7/24} N^{5/6} \quad (\text{i.e., } b = 7/24, c = 5/6).$$

Proceeding similarly for  $\phi(z) \sim g_{sol}/\xi_{sol}^3$ , we find that  $\phi(z) \sim \phi_0^{7/10}(a/z)^{2/5}$ , which is Guiselin's second result. Recent experiments by Auvray, Auroy, and Cruz (AAC) [13] on irreversible adsorption of PDMS on silica support these scaling results. Note that in Guiselin's study the layer is in contact with pure solvent only, not a bulk solution of polymers, as in our simulation. The effect of this difference is thought to be small in the limit of infinite adsorption strength. This is because the bulk chains do not penetrate the layer as they do in the case of finite adsorption strength [4], and so should have little effect on the layer. For this reason, we compare our

results with Guiselin's. Nevertheless, our present study does not exactly correspond to Guiselin's assumptions. For one thing, we allow the chains initially at the surface to adsorb more completely over time. We also allow the further adsorption of new chains. In this way, our quasiequilibrium profile actually occurs in a somewhat different phase of growth from the one studied by Guiselin. Using  $\phi_0^{actual}$  and our results for  $\langle z \rangle$  from Table III, we find  $b = 0.20 \pm 0.03$  and  $c = 0.81 \pm 0.05$ , which is in excellent agreement with Guiselin's first result. This agreement motivates us to plot  $\ln[\phi_{ads}(z)a^3]$  as a function of  $\ln(z)$  in Fig. 12, for all the system configurations studied. We also plot the slope corresponding to Guiselin's second result for comparison. The agreement is not very good, but not inconsistent with our data either. It may be that the predicted region is very short in the cases we consider.

A scaling study by Marques and Joanny [26] predicts that in a melt (or dense solution) the adsorbance should obey the scaling relation  $\Gamma \sim N^{1/2}\phi_0^{7/8}$ , which is supported by recent experimental results by Auvray, Cruz, and Auroy (ACA) [12] on irreversible adsorption of PDMS on silica. Marques and Joanny have also applied this result to semidilute solutions. This scaling result follows from writing

$$\Gamma \sim \Gamma^{ex} + \phi_0 R$$

where  $\Gamma^{ex}$  is the surface excess and  $R \sim N^{1/2}\phi_0^{-1/8}$ . The second term is an estimate of the adsorbance (here, the number of monomers in the adsorbed phase per unit area) due to chains initially present at the surface, i.e., between  $z = 0$  and  $z = R$ . It corresponds to the chains kept in Guiselin's study. In a melt,  $\phi_0 = 1$ , and this second term will be the dominant contribution to  $\Gamma$ , while the first can be neglected. It is in this case that the results of ACA agree with this relation. Although ACA focus mainly on this case, they also tabulate several results for lower concentration solutions, similar to our semidilute case. These results show a progressive decrease in these scaling exponents as the solution is made more dilute, and

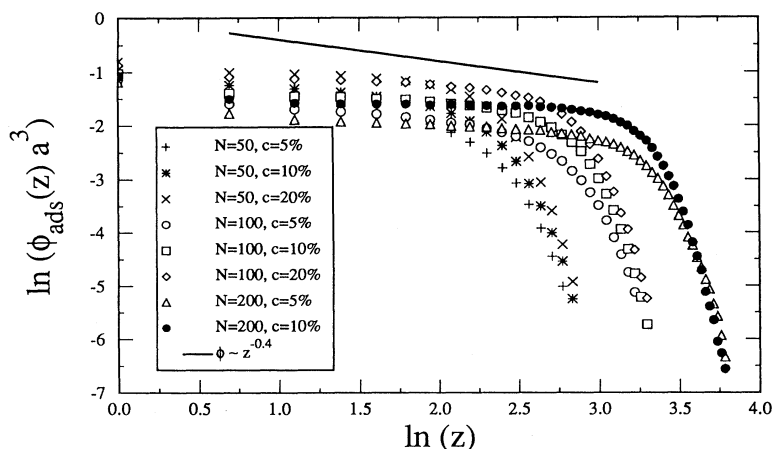


FIG. 12. Logarithmic plot of the total density profile of adsorbed chains, for the case of homopolymer adsorption. The solid line represents the slope corresponding to Guiselin's scaling prediction.

$\Gamma^{ez}$  becomes non-negligible. From our results, we find roughly that in this intermediate regime  $\Gamma \sim N^{0.38} \phi_0^{0.38}$ . These exponents are consistent with the experimental results of ACA for a 10% solution of the shortest chains they consider.

## V. CONCLUSIONS

We have studied the kinetics of growth of polymer chains adsorbing irreversibly to a surface from semidilute solutions. We have considered the cases of both end-functionalized polymer chains and adsorbing homopolymers. We have also studied the structure of the adsorbed layers at late times.

The growth of a layer of end-functionalized chains is found to be governed by diffusion of the chains at early times, hindered by interference from the existing layer which forms extremely quickly. Thus, the exponent of 0.5 characteristic of diffusion measures closer to 0.3 here. The growth quickly becomes logarithmic with the formation of an activation barrier, as predicted by Ligoure and Leibler. The incoming chains must expend some free energy in stretching to penetrate the brushlike layer, and this growth becomes slower with increasing chain length, matching Ligoure and Leibler's prediction. The resulting layer is found to be a strongly stretched brush, with a density profile similar to the parabola predicted by Milner, Witten, and Cates. We begin to see deviations from this parabola at higher solution concentrations, as the distribution becomes more closely packed in some regions, causing the profile to become flatter than a parabola. The free chains are found to be completely expelled from the region occupied by the brush, unlike in our previous study, where the significant free chain penetration is thought to be responsible for perturbing the shape of the density profile. The adsorbed profiles fall onto a master curve when lengths are rescaled by  $\langle z \rangle$ , the first moment of the brush, and  $\phi_{ads}(z)$  and  $\phi_{free}(z)$  are rescaled by their maximum values, respectively. This scaling works well throughout the growth of the brush, and at late times (quasiequilibrium) also. The scaling curve from our previous study does not match this one,

because of the total expulsion of the free chains from the region near the surface, and also because the dynamics in the present case are slightly different, not allowing the brush chains to slide along the surface.

The growth of a layer of irreversibly adsorbing homopolymers is found to proceed in three phases. In the first phase of growth, the number of vacant surface sites decays exponentially, as the coiled chains initially near the surface become adsorbed. Meanwhile, the total adsorbance  $\Gamma$  grows mainly through the same screened diffusion as in the case of end-functionalized chains. This diffusion continues through the second, crossover phase. In the third phase of growth, the further growth of the layer is dominated by a "reeling in" of the partially adsorbed chains, which becomes complicated for large chain lengths. During this final phase,  $\Gamma$  grows logarithmically, as incoming chains have a hard time penetrating the existing layer, and must stretch somewhat in order to poke through.

At late times, the layer comprises a number of loops near the surface, and tails extending further out. The density profile of the tails is parabolic, but the parabola's center is pushed outward by the loop distribution. This tail-dominated region of the profile behaves like a brush layer; it is responsible for the logarithmic growth of  $\Gamma$ , just as in the case of end adsorbing chains. The density profile of the loops behaves like an exponential decay a few lattice spacings away from the surface. The first moment of the whole layer  $\langle z \rangle$  is found to be consistent with Guiselin's prediction  $h \sim a\phi_0^{7/24} N^{5/6}$ , but his further prediction that the density profile should behave as  $\phi(z) \sim z^{-2/5}$  does not convincingly fit our limited amount of data.

## ACKNOWLEDGMENTS

We thank Dr. J. Marko, Professor C. Sorenson, and Professor W. Stevenson, for many useful discussions. This material is based upon work supported by the National Science Foundation under Grant No. OSR-9255223 (NSF-EPSCoR). This work also received matching support from the State of Kansas.

- 
- [1] W. B. Russel, D. A. Saville, and W. R. Schowalter, *Colloidal Dispersions* (Cambridge University Press, Cambridge, England, 1989).
  - [2] S. T. Milner, *Science* **251**, 905 (1991); A. Halperin, M. Tirrell, and T. P. Lodge, *Adv. Polym. Sci.* **100**, 31 (1991); G. Grest and M. Murat (unpublished).
  - [3] A. C. Balazs, M. C. Gempe, and C. W. Lantman, *Macromolecules* **24**, 168 (1991); A. C. Balazs, K. Huang, P. McElwain, and J. E. Brady, *ibid.* **24**, 714 (1991).
  - [4] R. Zajac and A. Chakrabarti, *Phys. Rev. E* **49**, 3069 (1994).
  - [5] P.-Y. Lai, *J. Chem. Phys.* **98**, 669 (1993).
  - [6] Y. Wang and W. L. Mattice, *Langmuir* **10**, 2281 (1994).
  - [7] O. Guiselin, *Europhys. Lett.* **17**, 225 (1992).
  - [8] M. Aubouy and E. Raphaël, *Macromolecules* **27**, 5182 (1994).
  - [9] M. Aubouy and E. R. J. M. di Meglio, *Europhys. Lett.* **24**, 87 (1993).
  - [10] J. P. Cohen-Addad, *Polymer* **30**, 1821 (1989); J. P. Cohen-Addad, C. Roby, and M. Sauviat, *ibid.* **26**, 1231 (1985); A. Viallat, J. P. Cohen-Addad, and A. Pouchelon, *ibid.* **27**, 843 (1986).
  - [11] K. Konstadinidis, Ph.D. thesis, University of Minnesota, 1992.
  - [12] L. Auvray, M. Cruz, and P. Auroy, *J. Phys. (France) II* **2**, 1133 (1992).
  - [13] L. Auvray, P. Auroy, and M. Cruz, *J. Phys. (France) I* **2**, 943 (1992).

- [14] S. T. Milner, T. A. Witten, and M. E. Cates, *Macromolecules* **21**, 2610 (1988).
- [15] S. Alexander, *J. Phys. (Paris)* **38**, 983 (1977).
- [16] P. G. de Gennes, *Adv. Colloid Interface Sci.* **27**, 189 (1987).
- [17] C. Ligoure and L. Leibler, *J. Phys. (Paris)* **51**, 1313 (1990).
- [18] P. G. de Gennes, *Macromolecules* **13**, 1069 (1980).
- [19] K. Kremer and K. Binder, *Comput. Phys. Rep.* **7**, 259 (1988).
- [20] It need not necessarily be a chemical bond to be irreversible. See, for example, Ref. [12]. However, in the case of a physical bond, sliding of the adsorbed monomers would be permitted.
- [21] A. Chakrabarti and R. Toral, *Macromolecules* **23**, 2016 (1990).
- [22] D. F. K. Shim and M. E. Cates, *J. Phys. (Paris) II* **50**, 3535 (1989).
- [23] P.-Y. Lai and K. Binder, *J. Chem. Phys.* **95**, 9288 (1991).
- [24] S. T. Milner, T. A. Witten, and M. E. Cates, *Macromolecules* **22**, 853 (1989).
- [25] P. G. de Gennes, *Scaling Concepts in Polymer Physics* (Cornell University Press, Ithaca, NY, 1979).
- [26] C. M. Marques and J. F. Joanny, *J. Phys. (Paris)* **49**, 1103 (1988).